Journal of Hazardous Materials 187 (2011) 348–354

Contents lists available at ScienceDirect

Journal of Hazardous Materials

journal homepage: www.elsevier.com/locate/jhazmat

Catalytic wet peroxide oxidation of azo dye (Direct Blue 15) using solvothermally synthesized copper hydroxide nitrate as catalyst

Yuzhong Zhan[a,*], Xiang Zhou[a,b], Bei Fu[a], Yiliang Chen[a]

[a] School of Chemical and Energy Engineering, Zhengzhou University, Kexue Road, Zhengzhou 450001, PR China
[b] Henan Xinlianxin Chemical Fertilizer Co., Ltd., Qinglong Road, Xinxiang 453700, PR China

ARTICLE INFO

Article history:
Received 3 September 2010
Received in revised form 3 January 2011
Accepted 9 January 2011
Available online 14 January 2011

Keywords:
Solvothermal synthesis
Copper hydroxide nitrate
Catalytic wet peroxide oxidation
Azo dye
Advanced oxidation process

ABSTRACT

Copper hydroxide nitrate ($Cu_2(OH)_3NO_3$) was synthesized solvothermally in anhydrous ethanol and characterized by XRD, FTIR, TG–DTA and SEM. The peroxide degradation of an azo dye (Direct Blue 15) on this material was evaluated by examining catalyst loading, initial pH, hydrogen peroxide dosage, initial dye concentration and temperature. The leaching of Cu from the copper hydroxide nitrate during the reaction was also measured. The copper hydroxide nitrate synthesized solvothermally, which was of a novel spherical morphology with complex secondary structures and contained high-dispersed Cu_2O impurity, showed good performance for oxidation degradation of the azo dye, especially high catalytic activity, high utilization of hydrogen peroxide and a wide pH range, whereas the copper hydroxide nitrate synthesized by the direct reaction of copper nitrate and sodium hydroxide showed low catalytic activity.

© 2011 Elsevier B.V. All rights reserved.

1. Introduction

Conventional biological wastewater treatment is usually ineffective in treating some industrial effluents containing pollutants such as dyes, phenol and its derivatives, pharmaceuticals and intermediates, and pesticides because these chemicals are biorefractory and toxic to microorganisms. Some physicochemical technologies, such as adsorption, coagulation, and membrane separation, have been used for the removal of various toxic pollutants, but these processes merely transfer pollutants from one medium to another requiring further treatment [1–3]. So-called advanced oxidation processes (AOPs), which are based on the generation of very active hydroxyl radicals, are becoming more and more important technologies for wastewater treatment. AOPs are especially used for treating toxic and biorefractory contaminates because these methods offer a potential of destructing toxic chemicals to water, carbon dioxide, and other harmless small molecules [4,5]. Among the various AOPs, the classical homogeneous Fenton process may be the most extensively studied system [6–8]. However, two major drawbacks exist in the process: the pH of operation should be strictly controlled around pH = 3; and large amounts of sludge require further treatment. To overcome these disadvantages, increasing attentions have been paid to research on the heterogeneous Fenton systems in recent years. However, up to now, the investigation of solid catalysts is limited to materials such as oxides of iron, Fe- and Cu-pillared clays, and Fe- and Cu-exchange zeolites, and little work has been done on other types of materials [9–12]. In order to obtain solid catalysts with more excellent performance, it is still necessary to test and develop novel catalytic materials. Recently, we reported that copper hydroxyphosphate ($Cu_2(OH)PO_4$), a basic copper salt without micropores or mesopores, showed considerable activity for oxidative degradation of an azo dye under near-neutral pH conditions [13]. Here we report the synthesis and catalytic properties about another basic copper salt, copper hydroxide nitrate ($Cu_2(OH)_3NO_3$).

$Cu_2(OH)_3NO_3$ is a layered compound and exists in two crystal types [14,15]. The natural $Cu_2(OH)_3NO_3$ named gerhardtite has an orthorhombic lattice, and it is slightly more stable than the synthetic $Cu_2(OH)_3NO_3$ which belongs to monoclinic crystal system. The crystal structure of both polymorphs is brucite-like and can be viewed as layers of Cu octahedra stacking upon each other. There exist two types of Cu octahedra: each Cu(1) atom is surrounded by four OH^- groups and two oxygen atoms belonging to NO_3^- groups; each Cu(2) atom is coordinated by four OH^- groups, the fifth OH^- standing at a greater distance, and an oxygen atom belonging to a NO_3^- group. The NO_3^- anions stand between the positive layers for charge balancing and are linked by hydrogen bonding to the OH^- groups belonging to the layers of Cu octahedra.

The NO_3^- anions located in the interlayer of $Cu_2(OH)_3NO_3$ structure are exchangeable. This character allows one to prepare novel layered materials with potential applications by anion-exchange reactions starting from $Cu_2(OH)_3NO_3$ [16–18]. Based on the sim-

* Corresponding author. Tel.: +86 371 67781025; fax: +86 371 67781025.
E-mail address: zhanyz@zzu.edu.cn (Y. Zhan).

0304-3894/$ – see front matter © 2011 Elsevier B.V. All rights reserved.
doi:10.1016/j.jhazmat.2011.01.027

ilar mechanism Park and Kim prepared $Cu(OH)_2$ nanorods by direct reaction of $Cu_2(OH)_3NO_3$ with aqueous NaOH solution at room temperature [19]. Very recently, Ischenko et al. reported that $Cu_2(OH)_3NO_3$ could enhance the catalytic activity of CO conversion [20]. This may be the only report on $Cu_2(OH)_3NO_3$ used directly as a catalyst.

Several methods have been developed for the synthesis of $Cu_2(OH)_3NO_3$. The most commonly used technique is the direct reaction of $Cu(NO_3)_2$ with NaOH aqueous solutions [15,21–23]. Urea can replace NaOH as the reactant because urea hydrolyzes to generate the OH^- ions required for the preparation [15,24]. However, these preparation methods can only be carried out in dilute solutions, and the experimental parameters should be strictly controlled to avoid the formation of $Cu(OH)_2$ and/or CuO [21]. Moreover, when urea is used the $Cu_2(OH)_3NO_3$ synthesized is easily contaminated by CO_3^{2-} ions [24]. $Cu_2(OH)_3NO_3$ can also be prepared by digesting CuO in $Cu(NO_3)_2$ concentrated aqueous solution at room temperature or an elevated temperature. This method usually requires very long reaction time (e.g., 10 days at 100 °C) [25,26]. Recently, Niu et al. prepared copper hydroxide nitrate microcrystals by the evaporation of $Cu(NO_3)_2$ solution in the absence of any surfactants or templates [27].

In the current work, we first synthesized $Cu_2(OH)_3NO_3$ solvothermally in anhydrous ethanol, and then evaluated the performance of catalytic wet peroxide oxidation. An azo dye, Direct Blue 15 (DB15), was used as a model pollutant. Effects of variables such as initial pH, catalyst loading, H_2O_2 dosage, initial dye concentration, and temperature were studied. The stability and Cu leaching from $Cu_2(OH)_3NO_3$ were also investigated. Surprisingly, the $Cu_2(OH)_3NO_3$ synthesized solvothermally showed high catalytic activity, whereas the control sample synthesized by the direct reaction of $Cu(NO_3)_2$ with NaOH according to the literature showed low activity in the catalytic wet peroxide oxidation of DB15.

2. Materials and methods

2.1. Materials

Direct Blue 15 (C.I. 24400), which purchased from Tianjin Shengda Chemical Plant (Tianjin, China), was of commercial grade and directly used without further purification. Its molecular structure is shown in Fig. 1. Other chemical reagents used were of analytical grade. All solutions were made in deionized water.

2.2. Synthesis and characterization of $Cu_2(OH)_3NO_3$

$Cu_2(OH)_3NO_3$ was synthesized solvothermally in anhydrous ethanol. A mixture containing 4.8 g $Cu(NO_3)_2{\cdot}3H_2O$, 0.8 g NH_4NO_3, and 60 mL anhydrous ethanol was stirred magnetically in a Teflon-lined stainless steel autoclave for 30 min, and then the autoclave was sealed. The crystallization was carried out at 150 °C for 48 h without stirring. The solid product was filtered, washed with water, and dried under vacuum at 80 °C for 8 h.

The control sample was synthesized by the direct reaction of $Cu(NO_3)_2$ with NaOH according to the literature [22]. The solid product was filtered, washed with water, and dried under vacuum at 80 °C for 8 h.

XRD data were collected on a Y-2000 automated X-ray diffractometer system (Dandong Aolong Radiative Instrument Co., Ltd., China) with Cu Kα radiation. FTIR spectra were obtained on a WQF-510 Fourier-transform infrared spectrometer (Beijing Rayleigh Analytical Instrument Corp., China) using the KBr disc method. SEM images were recorded on a JSM-5600LV (Jeol, Japan). The thermal analysis was carried out using a DTG-60 thermal analyzer (Shimadzu, Japan) in N_2 flowing atmosphere at a heating rate of 10 °C/min.

2.3. Batch experiments of dye decolorization

The catalytic degradation of dye was carried out in a 150 mL cylindrical jacketed glass reactor with magnetic stirring. The reaction temperature was controlled by circulating constant temperature water. In a typical run, a given amount of $Cu_2(OH)_3NO_3$ was added into 100 mL DB15 solution which has been adjusted to the desired pH by adding diluted NaOH or H_2SO_4. When the temperature was constant, the reaction was initiated by adding a known dosage of H_2O_2 (a 10-times diluted solution of 30% (w/w) H_2O_2) to the solution. At given time intervals 5 mL solution was taken out and centrifuged to remove the residual catalyst. The concentration of DB15 was measured using a SP-756PC UV–vis spectrophotometer (Shanghai Spectrum Instrument Co., Ltd., China) at 600 nm. The decolorization efficiency was used to describe the catalytic degradation of DB15, which was calculated by the following equation

$$\text{Decolorization efficiency} = \frac{A_0 - A_t}{A_0} \times 100\%$$

where A_0 is the initial absorbance, A_t is the absorbance at time t.

The amount of Cu leaching into the solution during the reaction was determined using a TAS-986 atomic absorption spectrometer (Beijing Purkinje General Instrument Co., Ltd.). The COD was measured spectrophotometrically according to a Chinese standard method (HJ/T 399-2007) by a DRB200 COD digester (Hach, USA) and a DR/2500 Spectrophotometer (Hach, USA). The possible interference of residual H_2O_2 was eliminated by adding a small amount of MnO_2 powder [28].

To study the effect of variables on degradation reaction, the experiments were repeated under different initial pH values (3.4–9.4), catalyst loading (0–150 mg), H_2O_2 dosage (0.1–1.0 mL), initial dye concentration (25–150 mg/L) and temperature (40–60 °C).

3. Results and discussion

3.1. Characterization of $Cu_2(OH)_3NO_3$

It should be emphasized that the color of the $Cu_2(OH)_3NO_3$ synthesized solvothermally is different from the control sample synthesized by the direct reaction of $Cu(NO_3)_2$ with NaOH according to the literature. The control sample was bluish-green and consistent with previous reports [15,22], whereas the $Cu_2(OH)_3NO_3$ synthesized solvothermally was dark brown. The dark brown color seems to imply the product being contaminated by some impurities (e.g., CuO and/or Cu_2O) because under solvothermal conditions copper salt may turn into CuO and CuO may be reduced to Cu_2O by ethanol [29]. However, no significant impurities were detected in the XRD analysis, as shown in Fig. 2. Nonetheless, through investigating the XRD pattern carefully we still found some evidence of the existence of high-dispersed Cu_2O in the $Cu_2(OH)_3NO_3$ synthesized solvothermally. Within the experimental range of 2-θ angle Cu_2O has three diffraction peaks locating at 29.6, 36.5 and 42.4° (JCPDS card File No. 65-3288). The very weak peak of Cu_2O at 29.6° was concealed by the peak of $Cu_2(OH)_3NO_3$. The peak at 36.5°, which should be the maximum peak of Cu_2O, was also concealed. But from the abnormal width of the peak bottom of $Cu_2(OH)_3NO_3$ we could presume the existence of Cu_2O peak. The peak at 43.4°, which should be a medium-strong peak of Cu_2O, could be recognized as a wide weak peak from the magnified XRD patterns. Apart from this, the diffraction peak positions of the as-synthesized $Cu_2(OH)_3NO_3$ were closely consistent with the

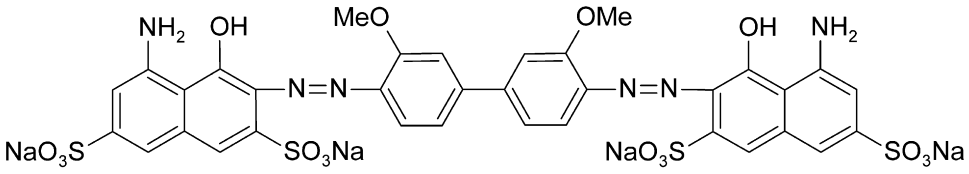

Fig. 1. The molecular structure of Direct Blue 15.

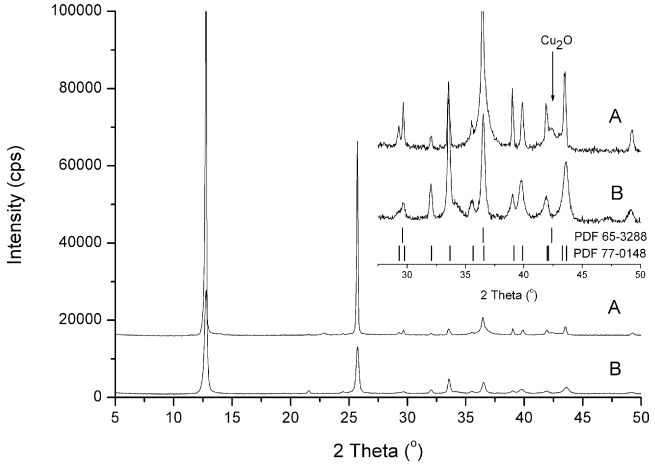

Fig. 2. XRD pattern of $Cu_2(OH)_3NO_3$ (A) synthesized solvothermally and (B) control sample.

control sample and the reported data (JCPDS card File No. 77-0148). Moreover, the $Cu_2(OH)_3NO_3$ as-synthesized showed a much better crystallinity because the peak intensity of XRD pattern was much higher than that of the control sample.

If the impurities exist in the as-synthesized $Cu_2(OH)_3NO_3$ as amorphous forms, the diffraction peaks will not be observed because XRD analysis can only detect crystal components. To obtain the further structural information of synthesized products the FTIR spectra of the as-synthesized $Cu_2(OH)_3NO_3$ and the control sample were measured, as shown in Fig. 3. Apparently, there were two extra peaks (at 1647 cm^{-1} and 629 cm^{-1}) in the FTIR spectrum of the as-synthesized $Cu_2(OH)_3NO_3$. The peak at 629 cm^{-1}, which was attributed to the stretching of Cu(I)–O, confirmed the presence of Cu_2O. The characteristic absorption peak of bulk Cu_2O was reported to be at 613 (±3) cm^{-1}. The absorption peak of Cu_2O nanomaterials reported was between 620 and 634 cm^{-1}. The slight shift in peak position could be the effect of reduction in particle size [30–34].

It is worthwhile to emphasize that no lattice water existed in the structure of the $Cu_2(OH)_3NO_3$ synthesized and dried by conventional methods [15,16,22]. However, the specific peaks of lattice water could be observed apparently in the FTIR spectrum of the $Cu_2(OH)_3NO_3$ synthesized solvothermally, in spite of the product being dried under vacuum at 80 °C for 8 h. The 1647 cm^{-1} peak could be assigned to H–O–H bending and the broadening of the absorption band at 3400–3500 cm^{-1} was due to the hydrogen bonds between the lattice water molecules [35]. Except these peaks associated with Cu_2O and lattice water, all other adsorption bands agreed well with the control sample.

The FTIR spectrum of the control sample agreed well with the literature in which the $Cu_2(OH)_3NO_3$ was synthesized by a controlled double jet precipitation of $Cu(NO_3)_2$ and NaOH, and dried in air at 60 °C overnight [15]. On comparing with Secco and Worth's detailed studies about the vibrational properties of this compound, we found that all adsorption peaks of the control sample could be assigned to the vibrations of groups associated with $Cu_2(OH)_3NO_3$ [25].

The TG–DTA curves of the $Cu_2(OH)_3NO_3$ synthesized solvothermally and the control sample are shown in Fig. 4. The control sample decomposed in one step producing CuO according to the chemical equation:

$$2Cu_2(OH)_3NO_3 = 4CuO + 3H_2O + 2NO_2 + (1/2)O_2$$

The total mass loss was 31.7%, which was close to the theoretical value of 33.7%. This result agreed well with the literature [15,17,23].

The results of thermal analysis of the $Cu_2(OH)_3NO_3$ synthesized solvothermally were very different with the control sample. Considering this material containing high-dispersed Cu_2O, we tried to give a reasonable interpretation. The exothermic peak at 310 °C was due to the oxidative reaction of Cu_2O to CuO. The required oxygen was provided by the decomposition of $Cu_2(OH)_3NO_3$ and the endothermic peak of the decomposition of $Cu_2(OH)_3NO_3$ was concealed. Another exothermic peak at 391 °C could be explained

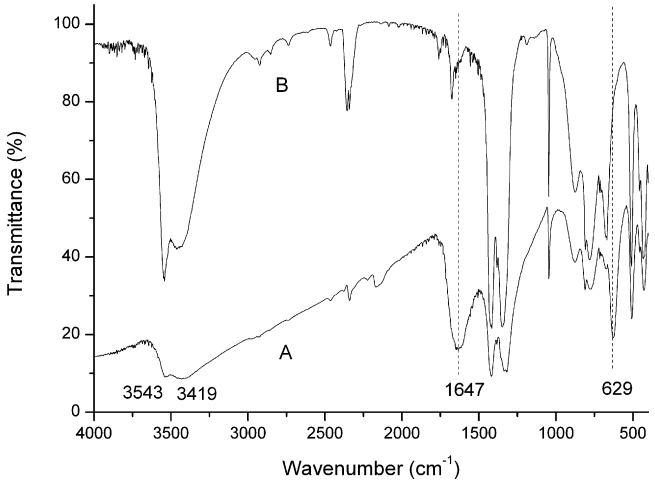

Fig. 3. FTIR spectra of $Cu_2(OH)_3NO_3$ (A) synthesized solvothermally and (B) control sample.

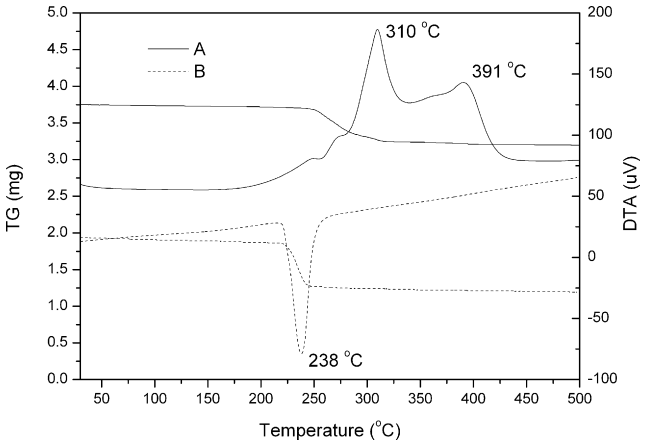

Fig. 4. TG–DTA curves of $Cu_2(OH)_3NO_3$ (A) synthesized solvothermally and (B) control sample.

as the further sintering of CuO, and this step did not result in the change in mass. The total mass loss was 12.4%, significantly lower than the theoretical value.

We also calcined the $Cu_2(OH)_3NO_3$ synthesized solvothermally at 400 °C for 2 h and the XRD result showed the calcined product was pure CuO phase (XRD pattern not shown).

Cu_2O is an important p-type semiconductor which can be used as a photocatalyst to degrade organic pollutions under visible light irradiation, but the research of Cu_2O as a Fenton-like catalyst without light irradiation has not been reported [29,32]. In copper-based Fenton-like heterogeneous system, such as CuO, Cu-pillared clays, and Cu-exchange zeolites as catalysts, Cu(II) is considered as the active species in general. However, according to the Fenton mechanism [36], the rate-limiting step is the reduction of Cu(II) by H_2O_2, then the resulting Cu(I) reacts with H_2O_2 directly to generate hydroxyl radicals. Consequently, the redox Cu(II)/Cu(I) cycle influences the catalytic activity significantly. The catalytic activity of $Cu_2(OH)_3NO_3$ synthesized solvothermally may be owing to the Cu_2O impurity which promotes the redox Cu(II)/Cu(I) cycle.

The SEM images of the $Cu_2(OH)_3NO_3$ synthesized solvothermally and the control sample are shown in Fig. 5. The morphology of the control sample was aggregates (5–50 μm in diameter) of hexagonal thin platelets, and it was similar to the earlier report [15,21]. However, the $Cu_2(OH)_3NO_3$ synthesized solvothermally showed a variety of crystal morphologies, and considerable parts of them were spherical morphology (5–30 μm in diameter) with complex secondary structures. The $Cu_2(OH)_3NO_3$ with these morphologies has not been reported previously.

Because the activity of catalyst is strongly dependent on its morphology and surface texture, the high catalytic activity of the $Cu_2(OH)_3NO_3$ synthesized solvothermally for degrading azo dye may also be related to its special morphology.

3.2. Effect of catalyst loading

Fig. 6 shows the effect of catalyst loading on the decolorization of DB15. To investigate the contribution of adsorption to the decolorization the control experiments in the absence of H_2O_2 were carried out firstly. The control sample showed some capacity of adsorption and the decolorization efficiency of DB15 reached 48.2% after 120 min when 100 mg catalyst loading was used. The adsorption capacity of the as-synthesized $Cu_2(OH)_3NO_3$ was lower than that of the control sample and the decolorization efficiency was 34.1% under the same condition. Another control experiment, in the absence of catalyst, showed that the decolorization efficiency was very low with only 5.5% after 120 min, indicating that the direct reaction of H_2O_2 with DB15 could be ignored. In the presence of H_2O_2 and the control sample (100 mg) the decolorization efficiency was 53.9%, only slightly higher than that in the absence of H_2O_2, showing a low catalytic activity for degrading dye. However, in the presence of H_2O_2 and the as-synthesized $Cu_2(OH)_3NO_3$ (100 mg) a significant decolorization could be observed. It indicated that this material showed high catalytic activity and greatly promoted the degradation of DB15 by H_2O_2. The decolorization efficiency reached 66.7% after only 5 min, and then it was 74.1 and 83.5% after 10 and 30 min, respectively. Further prolonging the reaction time the decolorization efficiency was almost constant, and it was 83.8% after 120 min.

As the catalyst loading increased to 150 mg the performance of decolorization was almost same with adding 100 mg catalyst. However, as the catalyst loading decreased to 50 mg a better performance of decolorization could be observed. The decolorization efficiency reached 62.4, 77.3, 87.8, and 90.1% when reaction time was 5, 10, 30, and 120 min, respectively. This phenomenon may be caused by several reasons. One reason is that due to the high catalytic activity the excessive catalyst may promote the decom-

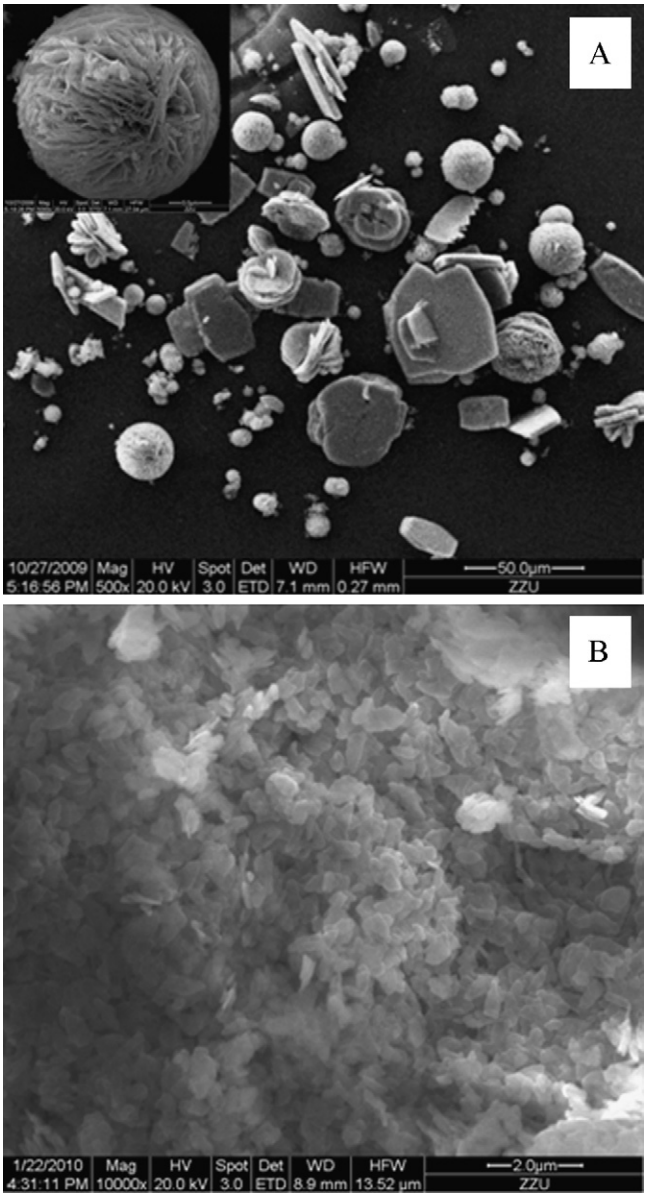

Fig. 5. SEM image of $Cu_2(OH)_3NO_3$ (A) synthesized solvothermally and (B) control sample.

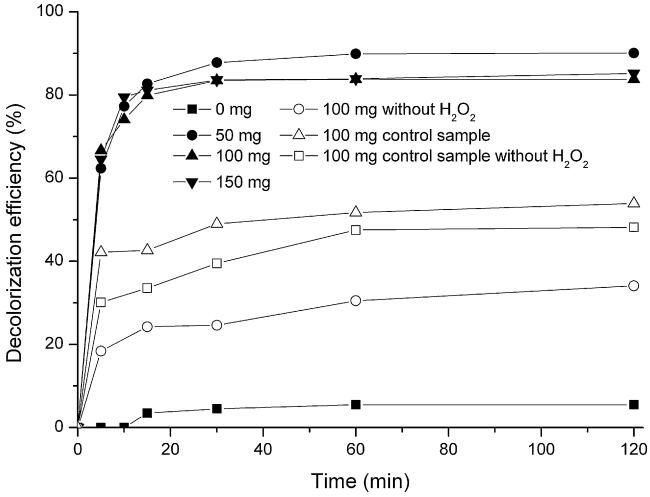

Fig. 6. Effect of catalyst loading on the catalytic degradation of Direct Blue 15 (pH = 6.7, DB15 100 mg/L, H_2O_2 0.5 mL, T = 50 °C).

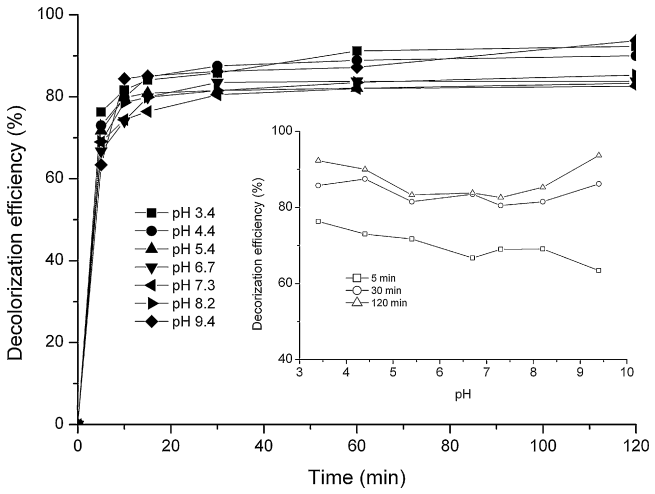

Fig. 7. Effect of initial pH on the catalytic degradation of Direct Blue 15 (DB15 100 mg/L, H_2O_2 0.5 mL, catalyst loading 100 mg, T = 50 °C). Inset: relationship of pH with Direct Blue 15 degradation at 5, 30, and 120 min, respectively.

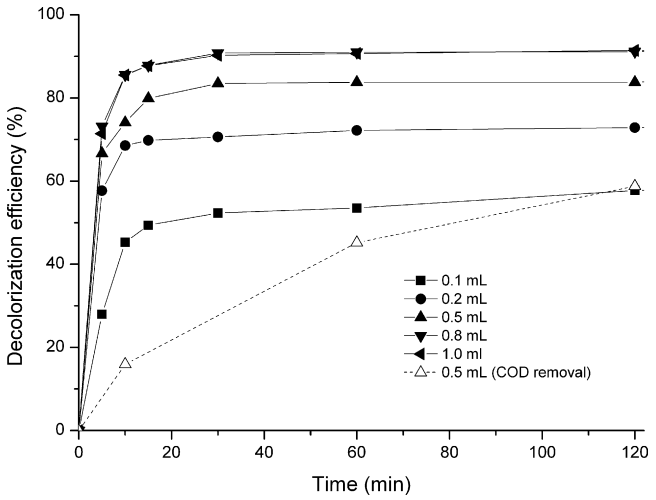

Fig. 8. Effect of H_2O_2 dosage on the catalytic degradation of Direct Blue 15 (pH = 6.7, DB15 100 mg/L, catalyst loading 100 mg, T = 50 °C).

position of H_2O_2, resulting in lower utilization of H_2O_2. In fact, we observed tiny bubbles releasing from the surface of catalyst at the initial stage of reaction. But we estimate that the decomposition is only a small percentage of H_2O_2 added and can be ignored. Another reason is that increasing the amount of the catalyst can accelerate the generation of hydroxyl radicals, and promote hydroxyl radicals reacting with the intermediates of dye degradation. Thus, the percentage of H_2O_2 used to react with dye itself resulting in the decolorization of dye may decrease in some degree.

3.3. Effect of initial pH

The effect of pH on the decolorization of dye was examined by adjusting the initial pH of DB15 solution in the range 3.4–9.4. It was found that the catalytic performance of the as-synthesized $Cu_2(OH)_3NO_3$ did not change significantly as varying the initial pH of the dye solution, as shown in Fig. 7. The decolorization in the first 5 min indicated that the initial rate of decolorization reaction slightly decreased as increasing pH from 3.4 to 9.4. However, the final decolorization after 120 min was only slightly lower at pH 5.4–8.2. Apparently, the as-synthesized $Cu_2(OH)_3NO_3$ could be used effectively at a much wider pH range. Because the operation under near-neutral conditions can easily apply to most wastewater and acidic conditions significantly enhance the leaching of active component, further experiments were carried out at pH 6.7, the natural pH value of DB15.

3.4. Effect of H_2O_2 dosage

The effect of H_2O_2 dosage on the degradation of dye is shown in Fig. 8. Because the H_2O_2 concentration is directly related to the number of hydroxyl radicals generated in the Fenton-like reaction, H_2O_2 dosage significantly influences the initial reaction rate. It could be noticed that when increasing the addition of H_2O_2 (a 10-times diluted solution of 30% (w/w) H_2O_2, the same below) from 0.1 mL to 0.8 mL the decolorization efficiency of dye went up from 28.0% to 73.1% at 5 min and from 57.8% to 91.2% at 120 min, respectively. When further increasing the addition of H_2O_2 to 1 mL the decolorization of the dye decreased slightly at 5 min and almost unchanged at 120 min comparing with the addition of 0.8 mL H_2O_2. This phenomenon is explained in general by the scavenging effect of excess H_2O_2, which decreases the number of hydroxyl radicals in the solution, so the addition of excess H_2O_2 results in a decrease in reaction rate [5,6,9,12]. But we suggest that increasing the addition of H_2O_2 promotes the generation of hydroxyl radicals and the hydroxyl radicals react with the intermediates of dye degradation, as mentioned above, because the addition of H_2O_2 was very small and the concentration of H_2O_2 in the reaction system was very low.

The overall stoichiometry for the complete degradation of DB15 by H_2O_2 can be written as:

$$C_{34}H_{24}N_6O_{16}SNa_4 + 93H_2O_2 = 34CO_2 + 100H_2O + 4NaHSO_4 + 6HNO_3$$

According to the above equation, 93 mol of H_2O_2 is theoretically needed to completely degrade 1 mol of Direct Blue 15. If 0.5 and 0.8 mL H_2O_2 were added into 100 mL Direct Blue 15 solution with the concentration of 100 mg/L, the calculated H_2O_2/dye molar ratios are 48.5 and 77.6, only about 52 and 83% of the theoretical value, respectively. As can be seen from Fig. 7, in such a low addition of H_2O_2, the decolorization of dye reached 83.8 and 91.2%, respectively, indicating a very high efficiency of H_2O_2 usage when using the as-synthesized $Cu_2(OH)_3NO_3$ as the catalyst. However, H_2O_2/pollutant molar ratios reported in the literature are usually much higher than the theoretical demand, meaning that a significant amount of H_2O_2 is not effectively used [11], and the same phenomenon also exists even in the heterogeneous photocatalytic degradation of organic pollutants [37].

The utilization of H_2O_2 is a very important indicator because it is directly related to the running costs of wastewater treatment. To further test the efficiency of H_2O_2 usage, the COD was measured when 0.5 mL H_2O_2 was added into 100 mL DB15 solution with the concentration of 100 mg/L. The calculation of COD removal efficiency was based on the theoretical oxygen demand of the complete mineralization of DB15, and the contribution of the blank experiment has been deducted. As shown in Fig. 8, the COD removal reached about 52% after 120 min, and it was consistent with the theoretical prediction. This result means that in this case the utilization of H_2O_2 may be almost up to 100%. On the other hand, the intermediate products of dye degradation are difficult to oxidise, and the complete destruction may proceed in a longer time.

3.5. Effect of initial dye concentration

The effect of initial dye concentrations on the degradation was investigated between 25 and 150 mg/L DB15 solutions as shown in Fig. 9. It was found that the final decolorization of dye decreased, whereas the initial rate of degradation significantly increased with the increase of dye concentration. The effect of dye

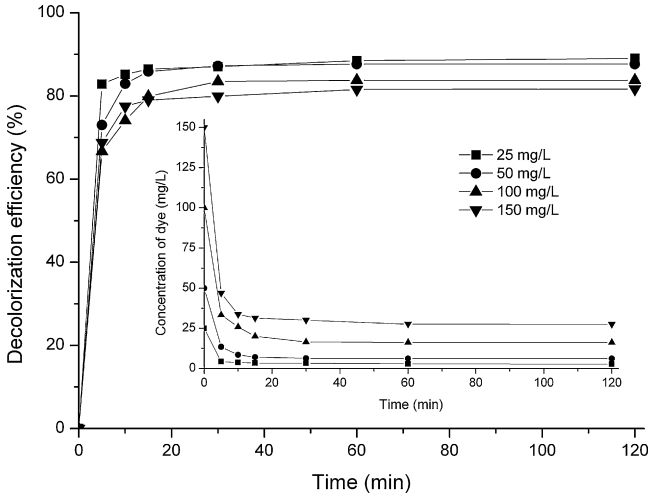

Fig. 9. Effect of initial dye concentration on the catalytic degradation of Direct Blue 15 (pH = 6.7, H_2O_2 0.5 mL, catalyst loading 100 mg, T = 50 °C). Inset: relationship of concentration of Direct Blue 15 with reaction time.

concentration on reaction rate agrees with the basic chemical principles, namely the increase of reactants concentration increases the collision frequency of molecules, and thus accelerates the reaction rate. Comparing with $Cu_2(OH)PO_4$, $Cu_2(OH)_3NO_3$ synthesized solvothermally showed more excellent performance because $Cu_2(OH)_3NO_3$ could degrade dye with higher concentration and gave higher rate of degradation.

3.6. Effect of temperature

The effect of temperature on the degradation reaction was investigated at 40, 50, and 60 °C. The results are given in Fig. 10. As expected, rising temperature increased the catalytic activity of degradation and the final decolorization efficiency. At 60 °C the degradation efficiency of DB15 reached about 85 and 90% after 10 and 60 min, respectively. Higher temperature not only increases energy consumption, but may result in decomposition of H_2O_2 thereby it reduces the efficiency of H_2O_2 usage.

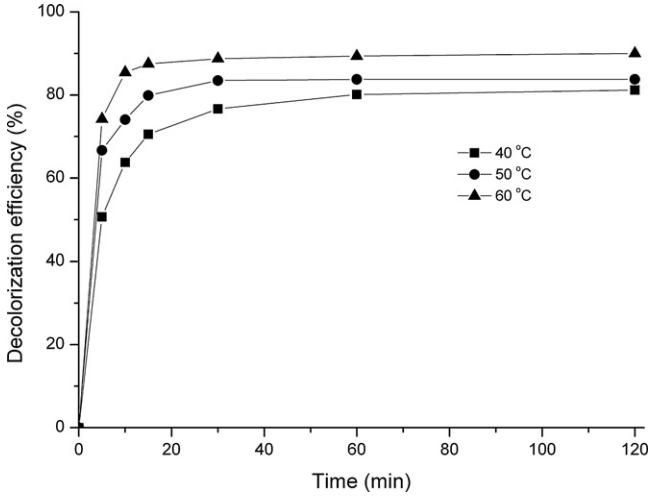

Fig. 10. Effect of temperature on the catalytic degradation of Direct Blue 15 (pH = 6.7, DB15 100 mg/L, H_2O_2 0.5 mL, catalyst loading 100 mg).

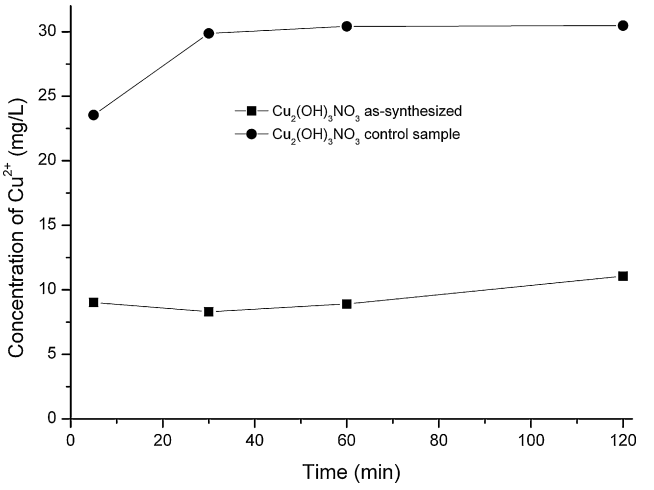

Fig. 11. Concentration of leaching Cu during the degradation of Direct Blue 15 (pH = 6.7, DB15 100 mg/L, H_2O_2 0.5 mL, catalyst loading 100 mg, T = 50 °C).

3.7. Stability of catalyst

The long-term stability of a catalyst is extremely essential for its industrial application. To evaluate the stability of the as-synthesized $Cu_2(OH)_3NO_3$, the Cu leaching during the reaction was measured. As shown in Fig. 11, the concentration of leaching Cu was almost constant at about 10 ppm after 5 min, and this was equivalent to a less than 2% loss of Cu component. As a comparison the concentration of leaching Cu of the control sample was about 30 ppm. To further evaluate the catalyst, a 12-h experiment was carried out. In this experiment the initial reaction system contained 100 mL DB15 (100 mg/L), 100 mg catalyst, and 0.5 mL H_2O_2. At every 2 h, 5 mL solution was taken out to be analyzed, and then 7 mg solid DB15 and 0.5 mL H_2O_2 was added into the reaction system. This process continued for 12 h, and the results are shown in Fig. 12. It was found that although the residual amount of DB15 increased with the reaction time, the accumulated decolorization efficiency of dye also increased, indicating the catalyst still maintained high catalytic activity. However, the final concentration of Cu measured reached about 40 ppm, indicating that the accumulation of acid intermediates significantly enhances the Cu leaching. So the Cu leaching of the as-synthesized $Cu_2(OH)_3NO_3$ cannot be ignored. Modified by partial ion exchange may be an appropriate strategy to stabilize this compound.

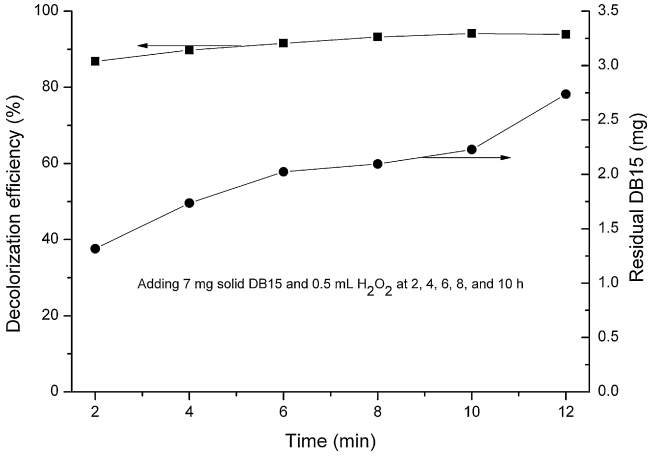

Fig. 12. Relationship of the decolorization efficiency and residual amount of Direct Blue 15 with reaction time (pH = 6.7, DB15 100 mg/L, H_2O_2 0.5 mL, catalyst loading 100 mg, T = 50 °C).

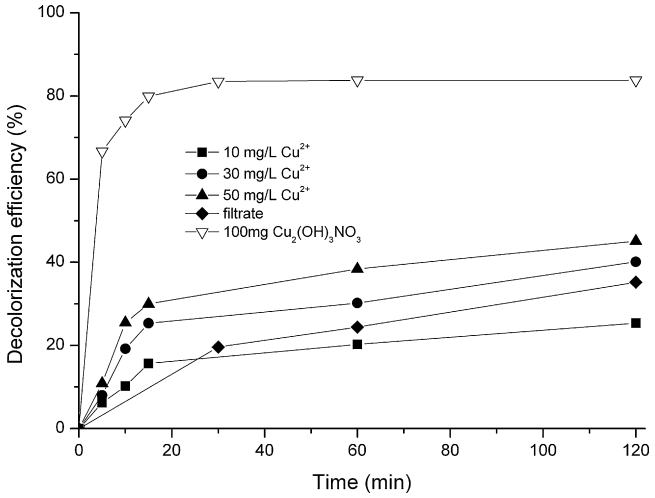

Fig. 13. Homogeneous catalytic degradation of Direct Blue 15 under various Cu^{2+} concentrations (pH = 6.7, DB15 100 mg/L, H_2O_2 0.5 mL, T = 50 °C).

As a comparison, we also tested the degradation of DB15 using Cu^{2+} (10, 30, and 50 mg/L, respectively) and the filtrate of degradation reaction as the homogeneous catalyst. Apparently, the catalytic activity of homogeneous Cu^{2+} is much lower than that of the as-synthesized $Cu_2(OH)_3NO_3$ as the catalyst under the same condition, as shown in Fig. 13. This may prove the heterogeneous catalysis of the as-synthesized $Cu_2(OH)_3NO_3$.

4. Conclusions

This paper described the synthesis, characterization, and catalytic behavior of the copper hydroxide nitrate synthesized solvothermally in anhydrous ethanol. This novel synthesis method resulted in a spherical morphology with complex secondary structures. This material showed good performance for oxidation degradation of azo dye (Direct Blue 15), especially high catalytic activity, high utilization of H_2O_2, and a wide pH range. In contrast, the copper hydroxide nitrate synthesized by the direct reaction of $Cu(NO_3)_2$ and NaOH aqueous solutions showed low catalytic activity for oxidation degradation of azo dye. The reason resulting in this difference may be owing to the high-dispersed Cu_2O impurity and their different morphology, but it is not clear. So in-depth studies for this material aiming at elucidating the nature of activity sites and the reaction mechanism are still necessary in the future.

Acknowledgment

The support of research grants from the Research Center of New Catalytic Materials is gratefully acknowledged.

References

[1] T. Robinson, G. McMullan, R. Marchant, P. Nigam, Remediation of dyes in textile effluent: a critical review on current treatment technologies with a proposed alternative, Bioresour. Technol. 77 (2001) 247–255.
[2] A. Chiavola, Textiles, Water Environ. Res. 81 (2009) 1696–1730.
[3] G. Buscaa, S. Berardinelli, C. Resini, L. Arrighi, Technologies for the removal of phenol from fluid streams: a short review of recent developments, J. Hazard. Mater. 160 (2008) 265–288.
[4] A. Vogelpohl, S.M. Kim, Advanced oxidation processes (AOPs) in wastewater treatment, J. Ind. Eng. Chem. 10 (2004) 33–40.
[5] M. Pera-Titus, V. García-Molina, M.A. Baños, J. Giménez, S. Esplugas, Degradation of chlorophenols by means of advanced oxidation processes: a general review, Appl. Catal. B 47 (2004) 219–256.
[6] E. Neyens, J. Baeyens, A review of classic Fenton's peroxidation as an advanced oxidation technique, J. Hazard. Mater. B98 (2003) 33–50.
[7] J.J. Pignatello, E. Oliveros, A. Mackay, Advanced oxidation processes for organic contaminant destruction based on the Fenton reaction and related chemistry, Crit. Rev. Environ. Sci. Technol. 36 (2006) 1–84.
[8] P. Bautista, A.F. Mohedano, J.A. Casas, J.A. Zazo, J.J. Rodriguez, An overview of the application of Fenton oxidation to industrial wastewaters treatment, J. Chem. Technol. Biotechnol. 83 (2008) 1323–1338.
[9] K. Pirkanniemi, M. Sillanpää, Heterogeneous water phase catalysis as an environmental application: a review, Chemosphere 48 (2002) 1047–1060.
[10] S. Perathoner, G. Centi, Wet hydrogen peroxide catalytic oxidation (WHPCO) of organic waste in agro-food and industrial streams, Top. Catal. 33 (2005) 207–224.
[11] L.F. Liotta, M. Gruttadauria, G. Di Carlo, G. Perrini, V. Librando, Heterogeneous catalytic degradation of phenolic substrates: catalysts activity, J. Hazard. Mater. 162 (2009) 588–606.
[12] E.G. Garrido-Ramírez, B.K.G. Theng, M.L. Mora, Clays and oxide minerals as catalysts and nanocatalysts in Fenton-like reactions – a review, Appl. Clay Sci. 47 (2010) 182–192.
[13] Y.Z. Zhan, H.L. Li, Y.L. Chen, Copper hydroxyphosphate as catalyst for the wet hydrogen peroxide oxidation of azo dyes, J. Hazard. Mater. 180 (2010) 481–485.
[14] B. Bovio, S. Locchi, Crystal structure of the orthorhombic basic copper nitrate, $Cu_2(OH)_3NO_3$, J. Crystallogr. Spectrosc. Res. 12 (1982) 507–517.
[15] C. Henrist, K. Traina, C. Hubert, G. Toussaint, A. Rulmont, R. Cloots, Study of the morphology of copper hydroxynitrate nanoplatelets obtained by controlled double jet precipitation and urea hydrolysis, J. Cryst. Growth 254 (2003) 176–187.
[16] S.H. Park, C.E. Lee, Layered copper hydroxide n-alkylsulfonate salts: synthesis, characterization, and magnetic behaviors in relation to the basal spacing, J. Phys. Chem. B 109 (2005) 1118–1124.
[17] G.G.C. Arizaga, K.G. Satyanarayana, F. Wypych, Layered hydroxide salts: synthesis, properties and potential applications, Solid State Ionics 178 (2007) 1143–1162.
[18] S.H. Park, C.E. Lee, Synthesis, characterization and magnetic properties of a novel disulfonate-pillared copper hydroxide $Cu_2(OH)_3(DS4)_{1/2}$, DS4 = 1,4-butanedisulfonate, Bull. Korean Chem. Soc. 27 (2006) 1587–1592.
[19] S.H. Park, H.J. Kim, Unidirectionally aligned copper hydroxide crystalline nanorods from two-dimensional copper hydroxy nitrate, J. Am. Chem. Soc. 126 (2004) 14368–14369.
[20] E.V. Ischenko, L.Y. Matzui, S.V. Gayday, L.L. Vovchenko, T.V. Kartashova, V.V. Lisnyak, Thermo-exfoliated graphite containing $CuO/Cu_2(OH)_3NO_3$:(Co^{2+}/Fe^{3+}) composites: preparation, characterization and catalytic performance in CO conversion, Materials 3 (2010) 572–584.
[21] S.H. Lee, Y.S. Her, E. Matijevic, Preparation and growth mechanism of uniform colloidal copper, oxide by the controlled double-jet precipitation, J. Colloid Interface Sci. 186 (1997) 193–202.
[22] S.P. Newman, W. Jones, Comparative study of some layered hydroxide salts containing exchangeable interlayer anions, J. Solid State Chem. 148 (1999) 26–40.
[23] D.C. Pereira, D.L. de Faria, V.R.L. Constantino, Cu^{II} hydroxy salts: characterization of layered compounds by vibrational spectroscopy, J. Braz. Chem. Soc. 17 (2006) 1651–1657.
[24] S. Kratohvil, E. Matijević, Preparation of copper compounds of different compositions and particle morphologies, J. Mater. Res. 6 (1991) 766–777.
[25] E.A. Secco, G.G. Worth, Infrared spectra of unannealed and of annealed $Cu_4(OH)_6(NO_3)_2$, Can. J. Chem. 65 (1987) 2504–2508.
[26] M. Meyn, K. Beneke, C. Lagaly, Anion-exchange reactions of hydroxy double salts, Inorg. Chem. 32 (1993) 1209–1215.
[27] H.X. Niu, Q. Yang, K.B. Tang, A new route to copper nitrate hydroxide microcrystals, Mater. Sci. Eng. B 135 (2006) 172–175.
[28] R.M. Liou, S.H. Chen, CuO impregnated activated carbon for catalytic wet peroxide oxidation of phenol, J. Hazard. Mater. 172 (2009) 498–506.
[29] M.Z. Wei, N. Lun, X.C. Ma, S.L. Wen, A simple solvothermal reduction route to copper and cuprous oxide, Mater. Lett. 61 (2007) 2147–2150.
[30] K. Borgohain, N. Murase, S. Mahamuni, Synthesis and properties of Cu_2O quantum particles, J. Appl. Phys. 92 (2002) 1292–1297.
[31] I. Prakash, P. Muralidharan, N. Nallamuthu, M. Venkateswarlu, N. Satyanarayana, Preparation and characterization of nanocrystallite size cuprous oxide, Mater. Res. Bull. 42 (2007) 1619–1624.
[32] Z.C. Orel, A. Anžlovar, G. Dražić, M. Žigon, Cuprous oxide nanowires prepared by an additive-free polyol process, Cryst. Growth Des. 7 (2007) 453–458.
[33] W.T. Wu, Y.S. Wang, L. Shi, W.M. Pang, Q.R. Zhu, G.Y. Xu, F. Lu, Propeller-like multicomponent microstructures: self-assemblies of nanoparticles of poly(vinyl alcohol)-coated Ag and/or Cu_2O, J. Phys. Chem. B 110 (2006) 14702–14708.
[34] Y.Y. Xu, D.R. Chen, X.L. Jiao, K.Y. Xue, Nanosized Cu_2O/PEG400 composite hollow spheres with mesoporous shells, J. Phys. Chem. C 111 (2007) 16284–16289.
[35] K. Nakamoto, Infrared and Raman Spectra of Inorganic and Coordination Compounds, Part B, Applications in Coordination, Organometallic, and Bioinorganic Chemistry, 6th ed., John Wiley & Sons, Inc., Hoboken, New Jersey, 2009.
[36] J.I. Nieto-Juarez, K. Pierzchła, A. Sienkiewicz, T. Kohn, Inactivation of MS2 coliphage in Fenton and Fenton-like systems: role of transition metals, hydrogen peroxide and sunlight, Environ. Sci. Technol. 44 (2010) 3351–3356.
[37] M. Bobu, A. Yediler, I. Siminiceanu, S. Schulte-Hostede, Degradation studies of ciprofloxacin on a pillared iron catalyst, Appl. Catal. B 83 (2008) 15–23.